11th World Congress on Structural and Multidisciplinary Optimization
7th - 12th, June 2015, Sydney Australia

An Immersed Boundary Approach for Sensitivity Analysis of Fluid-structure Interactions

Ramana V. Grandhi[1], Koorosh Gobal[2]

[1] Wright State University, Dayton, Ohio, ramana.grandhi@wright.edu
[2] Wright State University, Dayton, Ohio, gobal.2@wright.edu

1. Abstract
Gradient-based optimization algorithms are highly advantageous for computer intensive simulations such as fluid-structure interaction (FSI) problems. Typical simulation involves solution of the Navier-Stokes equations and their response sensitivities. Due to the use of body conformal meshes, mesh topology modification is required in structural shape optimization; however, this can be time consuming for complex structural boundaries. In this research, we introduce a method based on adding force terms to the Navier-Stokes equations to decouple the solid boundary definition from the mesh. Therefore, the governing equations can be solved on a Cartesian grid with efficient solvers. Decoupling the solid boundary from the mesh enables us to deform the solid domain without mesh modification allowing a significant reduction in computational costs. To calculate the sensitivity response of the system, the continuum sensitivity method is developed. Force terms are used to represent the solid boundaries and convective terms are removed in boundary conditions sensitivity equations because the boundaries do not depend on domain configuration. The methodology is verified using the sensitivity of laminar flow over a Joukowsky airfoil with respect to change in camber radius. The force terms are applied using the regularized Heaviside function to satisfy the no-slip condition in the solid domain.
2. Keywords: Fluid-solid interaction, Sensitivity analysis, Immersed boundary method.

3. Introduction

The analytical methods for calculating the design sensitivities can be divided into discrete and continuum methods. In the discrete method, the continuous governing equations are discretized and then differentiated resulting in equations that govern the sensitivity of responses [1]. However, discrete methods require the modification of the source-code of the black-box CFD/FEA solvers. This might not be possible due to the unavailability and complexity of the solver [2].

Continuum sensitivity analysis (CSA) involves solving a set of partial differential equations called the continuum sensitivity equations (CSEs). Choi and Kim developed the CSA formulation extensively for structural optimization [3]. Pelletier and Etienne have applied CSA to fluid-structure interaction (FSI) problems [4]. Liu and Canfield [5] used the finite element method to solve the potential flow around an airfoil and applied CSA to find the sensitivity of the solution to the airfoil's maximum camber. These works are built around using body-conformal meshes to discretize the domain. Since the shape of the immersed structure can change, mesh deformation algorithms are required to generate a new mesh that can be utilized to calculate the new response of the system. Mesh deformation and boundary movement are also reflected in the definition of boundary conditions for the CSEs [5].

Mesh deformation schemes are separated into algebraic and elasticity-based methods. Algebraic mesh movement methods are efficient but limited to small changes in shape [6]. Elasticity methods, including the spring analogy, are based on continuum mechanics. The use of spring analogy can result in tangled meshes and negative cell volumes, particularly for large deformations. To enhance the robustness of the scheme, nonlinear torsional stiffness has been introduced to mesh nodes; however, this increases the required computational cost.

Body conformal meshes require the computational mesh to contact all the boundaries, resulting in the dependence of mesh topology on the shape of the immersed body. By decoupling the boundary definition from the mesh topology, the mesh deformation step can be removed from the solution scheme. Moreover, the boundary conditions for the CSEs will be greatly simplified. This can be achieved by using the body-force terms in the Navier-Stokes equations in such a way that the effect of immersed bodies can be captured within the governing equation. Since the immersed boundary effect is included in the governing equation, its shape can be modified without changing the topology of the computational mesh. The effect of certain boundary conditions can be modeled with an external force field rather than with specification of boundary parameter values. The immersed boundary method uses this technique to decouple the solid and fluid domains. The term immersed boundary (IB) method refers to techniques that simulate viscous flows with immersed boundaries on grids that do not conform to the shape of the immersed boundaries [7].

In this research, we use the idea of IB method to add force terms to the governing equations. The force term is responsible for generating the pressure drop which represents the existence of solid boundaries in the domain. This approach is in contrast to the usual IB method that uses the velocity data to calculate the required force terms. Moreover, the force terms are linearly related to the flow parameters and no extra effort is needed to calculate them. The force terms are added to the governing equations using a regularized Heaviside function [8] which defines the boundary contour of the solid region. This is similar to a smooth representation of a step function. Regularized Heaviside functions are widely used in the topology optimization community as filters to eliminate checkerboards and mesh-dependencies. This is in contrast to their application in this paper, where they are functions of space [9].

4. Numerical Method

The Navier-Stokes equations permit the presence of an externally imposed body force that may vary in space and time. The force term is used to introduce the pressure drop that is proportional to the velocity of each point. The Navier-Stokes equation with body force S_i is defined as

$$\frac{\partial}{\partial t}(\rho u_i) + u_j \frac{\partial}{\partial x_j}(\rho u_i) = -\frac{\partial p}{\partial x_i} + \mu \frac{\partial \tau_{ij}}{\partial x_j} + S_i \tag{1}$$

with the force term

$$S_i = -\mu D u_i \cdot H\left[\mathscr{C}(\mathbf{x})\right] \tag{2}$$

where $\mathscr{C}$ is the contour representation of the boundary of the solid region. The regularized Heaviside function, H, is used to assign the force term, S_i, to the regions within the contour represented by $\mathscr{C}$. Using this method, the shape of the solid domain is modified through changing the location of force terms which does not change the mesh topology.

In this formulation, the zero velocity (no-slip condition) is satisfied both inside and also on the surface of the solid boundary contour. The force terms are defined with no extra interpolation from the the velocity field. This also adds to the simplicity of the method compared to the IB techniques where a further interpolation is usually required for calculating the force terms. It is also noteworthy to mention that the force terms are calculated at the same time as the velocity components; therefore, no extra cost is introduced in the solution of the discretized governing equations.

For a two-dimensional case, curve $\mathscr{C}$, is a non-self-intersecting continuous loop that defines the boundary of the solid region. The technique used for assigning the force term to mesh cells needs to be differentiable since the governing equation (1) is differentiated for deriving the CSEs. To satisfy these requirements, the regularized Heaviside function is used to assign the force terms. Different regularized Heaviside functions used in the literature are shown in Figure 1.

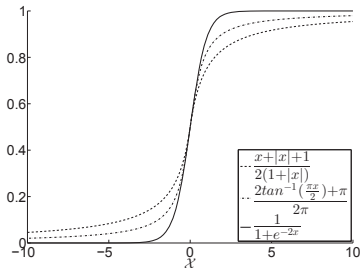

Figure 1: Comparison between different regularized Heaviside functions.

In this work, the regularized Heaviside function shown below is used due to its fast transition from zero to one.

$$H(\mathscr{X}) = \frac{1}{1+e^{-\kappa \mathscr{X}}} \tag{3}$$

As shown in Figure 1, the regularized Heaviside function, $H(\mathscr{X})$, gives one for positive values of $\mathscr{X}$ and zero otherwise. The positive and negative values of $\mathscr{X}$ correspond to cells outside and inside the solid boundary curve. It should be noted that near the boundary, there is a transition region where the value of the regularized Heaviside function is between zero and one. Therefore, it introduces error in the simulation result by generating unrealistic

pressure drop in the domain. These cells are known as *gray cells* in the topology optimization community. One way to alleviate this problem is to force the transition region to occur within one cell. This is done by modifying the Heaviside function as shown in Figure 2.

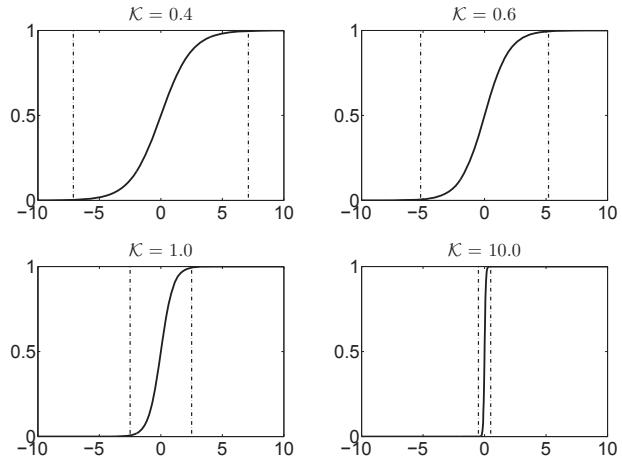

Figure 2: Effect of modifying the regularized Heaviside function in the transition region.

It should be noted that the center of each cell defines its location with respect to the solid boundary curve. Because the force terms are assigned to each volume, it is not possible to capture the exact boundary curve on a coarser mesh. However, by refining the mesh near the boundary curve, the effect of curvature can be captured almost completely on the solution of the problem.

Consider the following general, nonlinear boundary value system defined in a domain Ω with a boundary Γ

$$\mathscr{A}(u, L(u)) = f(x,t;b) \tag{4}$$

with boundary conditions defined as

$$\mathscr{B}(u, L(u)) = g(x,t;b) \quad \text{on } \Gamma \tag{5}$$

for which we seek a solution $u(x,t;b)$. In the above equation, $u = u(x,t;b)$ is dependent on design variable b implicitly and L is a linear differential operator, such as $\dfrac{\partial}{\partial x_i}$, that appears in the governing differential equations or boundary conditions. $\mathscr{A}$ and $\mathscr{B}$ are vectors of algebraic functions of u and $L(u)$. $\mathscr{B}(u, L(u))$ can be a simple function of u, such as a prescribed boundary condition for Dirichlet boundary conditions, or involve a differential operator for Neumann boundary conditions.

The CSE is formulated by directly differentiating the governing equations of Equation (4) as shown below where $u' = \dfrac{\partial u}{\partial b}$.

$$\frac{\partial \mathscr{A}}{\partial u} u' + \frac{\partial \mathscr{A}}{\partial L} L(u') = \frac{\partial f(x,t;b)}{\partial b} \tag{6}$$

For a problem with moving boundaries, the boundary conditions for Equation (6) can be derived by taking the total derivative of boundary condition Equation (5). The total derivative is needed here because the shape of boundaries can change [5]. This arises mostly when calculating the sensitivities due to change in shape of the domain. The total derivative is written as

$$\frac{Du}{Db} = \frac{\partial u}{\partial b} + \frac{\partial u}{\partial x}\frac{\partial x}{\partial b} \tag{7}$$

where $\dfrac{\partial x}{\partial b}$ is the geometric sensitivity or design velocity, which is dependent on domain parameterization. After taking the total derivative of Equation (5), the CSE boundary conditions are written as

$$\frac{\partial \mathscr{B}}{\partial u} u' + \frac{\partial \mathscr{B}}{\partial L} L(u') = \dot{g}(x,t;b) - \frac{\partial x}{\partial b} \cdot \left(\frac{\partial \mathscr{B}}{\partial u}\frac{\partial u}{\partial x} + \frac{\partial \mathscr{B}}{\partial L} L\left(\frac{\partial u}{\partial x}\right)\right) \tag{8}$$

where $\dot{g}(x,t;b)$ is the material derivative of the boundary condition. Within the scope of this paper, the boundary conditions are only applied at the outer part of the computational domain. It is assumed that these boundaries are independent of the domain configuration and their locations are not affected by the design variables. This is a valid assumption because the outer boundary conditions are typically defined as *far-field* values for flow-field variables(i.e. velocity and pressure, or their gradients). Their locations do not change and the design sensitivity is equal to zero at the boundaries; therefore, the material and local derivatives are equal on the boundaries. Equation (8) can be simplified as

$$\frac{\partial \mathscr{B}}{\partial u}u' + \frac{\partial \mathscr{B}}{\partial L}L(u') = g'(x,t;b) \tag{9}$$

The CSE of Equation (6) with the boundary conditions given in Equation (9) is a well posed system of equations in terms of sensitivity variable u' that can be solved using same numerical method used for solving the analysis problem. The spatial gradient of u in Equation (9) can be found from the solution of governing equation (4).

5. Demonstration Results

Laminar flow over a Joukowsky airfoil is selected to verify the methodology. The fluid-solid interaction is defined by mounting the airfoil on an elastic sting. The load and moment from the aerodynamic loads are transferred to the structure through the mounting point. The sting is 4 m in length, with a cross-sectional area of 0.002 m^2, and modulus of elasticity of 200 GPa. The initial angle of attack is selected at 8 degrees with a freestream velocity of 26 m/s. This gives the Reynolds number of 2600 for this simulation.

The airfoil is defined using the Joukowsky transformation shown in Equation (10), it is possible to map a circle passing through $z_1 = 1$ and containing the point $z_2 = -1$ to a curve shaped like the cross section of an airplane wing. The Joukowsky transformation is done in a complex plane.

$$J(z) = z + \frac{1}{z} \tag{10}$$

By changing the location of the original circle, it is possible to change the airfoil camber. More importantly, the airfoils have analytical definition that will be used in imposition of the force terms to the mesh cells. The effect of change in the location of original circle to the camber of the airfoil is shown in Figure 3. It should be noted that after generation, the airfoils are normalized such that the chord length is always equal to one.

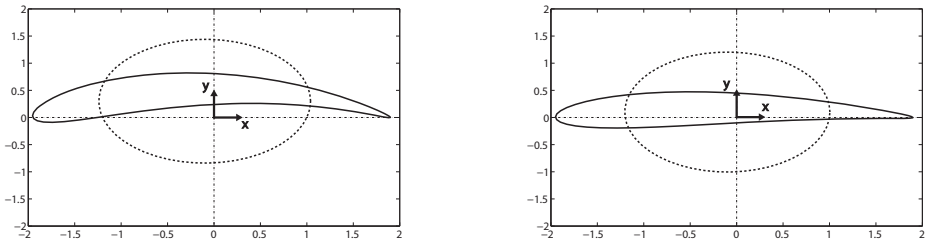

(a) Original circle at $(-0.1, 0.3)$ (b) Original circle at $(-0.1, 0.1)$

Figure 3: Airfoil definition by Joukowsky transformation (not normalized).

The governing equations, along with the boundary conditions, are differentiated to derive the CSEs. The resulting system of equations is solved to get the sensitivity response of the system. As shown in Figure 3, the y coordinate of the center of the original circle defines the camber. Thus, the sensitivity of the pressure field to airfoil's camber can be calculated by differentiating the governing equation by the y coordinate of the center of the original circle (design variable, b).

The differentiated governing equations can be written as

$$u\frac{\partial \mathscr{U}}{\partial x} + v\frac{\partial \mathscr{U}}{\partial y} = -\frac{\partial \mathscr{P}}{\partial x} + \mu\left[\frac{\partial^2 \mathscr{U}}{\partial x^2} + \frac{\partial^2 \mathscr{U}}{\partial y^2}\right] + \frac{\partial S_x}{\partial b} - \mathscr{U}\frac{\partial u}{\partial x} - \mathscr{V}\frac{\partial u}{\partial y} \tag{11a}$$

$$u\frac{\partial \mathscr{V}}{\partial x} + v\frac{\partial \mathscr{V}}{\partial y} = -\frac{\partial \mathscr{P}}{\partial y} + \mu\left[\frac{\partial^2 \mathscr{V}}{\partial x^2} + \frac{\partial^2 \mathscr{V}}{\partial y^2}\right] + \frac{\partial S_y}{\partial b} - \mathscr{U}\frac{\partial v}{\partial x} - \mathscr{V}\frac{\partial v}{\partial y} \tag{11b}$$

$$\frac{\partial \mathscr{U}}{\partial x} + \frac{\partial \mathscr{V}}{\partial y} = 0 \tag{11c}$$

where $\mathscr{U} = \dfrac{\partial u}{\partial b}$, $\mathscr{V} = \dfrac{\partial v}{\partial b}$, and $\mathscr{P} = \dfrac{\partial p}{\partial b}$. The values for u and v (velocity components in x and y direction) are known from the solution of governing equations. Furthermore, the spatial gradients of u and v are calculated via the QUICK scheme using the surrounding cell data. This is the same method that is used for discretizing the spatial gradients in the governing equations. The QUICK scheme is based on a quadratic function and has third order accuracy on a uniform mesh.

The derivative of the force terms on the right hand side of Equation (11) has the following form.

$$\frac{\partial S_x}{\partial b} = -\mu \mathscr{U} DH(\mathscr{X}, b) - \mu u D \frac{\partial H(\mathscr{X}, b)}{\partial b} \tag{12a}$$

$$\frac{\partial S_y}{\partial b} = -\mu \mathscr{V} DH(\mathscr{X}, b) - \mu v D \frac{\partial H(\mathscr{X}, b)}{\partial b} \tag{12b}$$

In the above equations, the derivative of the regularized Heaviside function introduces the effect of shape change in the solution of the sensitivity equations. In previous works [5], this was included in the boundary condition definition through convective terms. Boundary conditions are selected independently from the configuration of the domain. Therefore, the specified values for the CSE boundary condition are assigned as zero values. It should be noted that the derivative of shape boundaries to design variable, b, is buried in the derivative of the Heaviside function. This can be calculated analytically by using the chain rule on Equations (10) and (3).

Comparing Equations (11) and (1), it is evident that the same solver can be used for solving both systems of governing equations; the difference is in adding additional source terms to Equation (1). It should be noted that this does not affect the numerical method used to solve the problem as these terms can be incorporated in the body force terms. The solution of Equation (1) is used for initializing the convective terms, i.e. u and v, in Equation (11). This results in faster convergence of the sensitivity solution compared to the governing equations. The sensitivity of pressure around an airfoil based on original circle location at $(-0.1, 0.1)$ is shown in Figure 5.

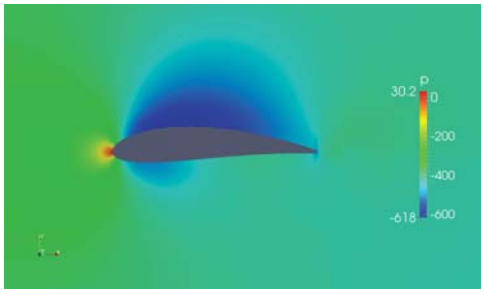

(a) Pressure contours for original circle at $(-0.1, 0.1)$

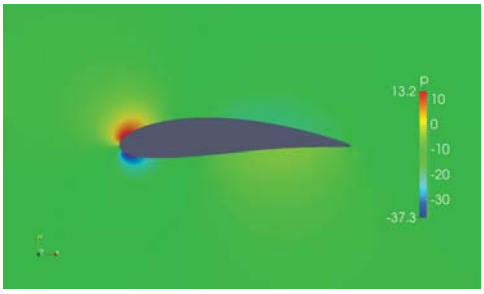

(b) Pressure sensitivity contours for original circle at $(-0.1, 0.1)$

Figure 4: Sensitivity of pressure field around airfoil to camber line variation.

The sensitivity of pressure field on top and bottom surfaces of the airfoil to camber line variation is shown in Figure 5. It should me noted that the method of moving average with 4 points is used to further smoothen the data over the boundaries.

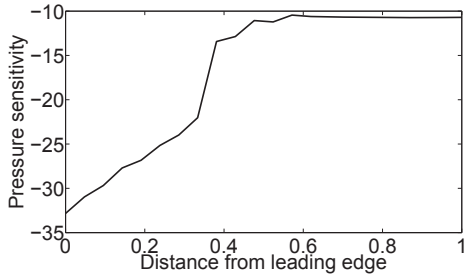

(a) Pressure sensitivity on the bottom surface

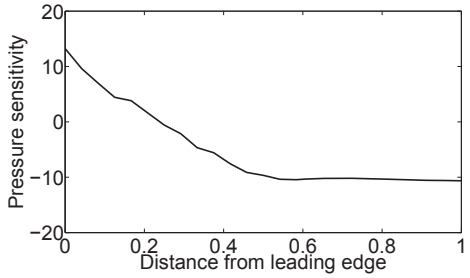

(b) Pressure sensitivity on the top surface

Figure 5: Sensitivity of pressure field on airfoil surface to camber line variation.

6. Conclusions

In this work, force terms are added to the Navier-Stokes equations to represent the solid boundaries inside the domain. The force terms act as a high pressure drop that results in satisfying the no-slip boundary condition in the solid domain. Using this method, it is possible to decouple the definition of solid boundary from the computational mesh; therefore, it is not required to deform the mesh topology when the solid boundary shape changes. Moreover, using this method, the governing equations are solved on a Cartesian structured grid where efficient solvers can be utilized. This reduces the computational time and memory requirements for the simulations.

The regularized Heaviside function is used to apply the force terms on the mesh volumes. Several regularized Heaviside functions are introduced and a model with the fastest transition is selected. One of the problems of using the regularized Heaviside function is the gray region within the domain and the numerical error associated with it. To remove the gray-cells from the computational domain, the regularized Heaviside function is forced to have a transition region within one cell. Using this approach, errors from the existence of gray-cells are minimized within the domain. The noise is further reduced by using the method of moving average when reporting the results on immersed boundary surfaces.

The continuum sensitivity equations are derived by differentiating the governing equations and their corresponding boundary conditions. In this approach, the interface boundary conditions are removed from the simulation by introducing the force terms. The outer boundary conditions usually do not depend on the domain configuration. Therefore, in most cases, the boundary conditions will be zero for sensitivity analysis using this approach. On the other hand, the effect of shape change is introduced to the domain through the derivative of the regularized Heaviside function. This acts as an additional force term in the governing equations. These equations have the same structure as the original governing equations and they can be solved using the same solver.

The applicability of this method is investigated by solving the flow and the sensitivity response of the laminar flow over a Joukowsky airfoil. The requirement of mesh deformation and use of body conformal mesh are removed from the simulation, which can save a significant amount of computational time and resources for conducting optimization.

6. References

[1] Martins, J. R. and Hwang, J. T., Review and unification of methods for computing derivatives of multidisciplinary computational models, *AIAA Journal*, Vol. 51, No. 11, 2013, pp. 2582-2599.

[2] Peter, J. E. and Dwight, R. P., Numerical sensitivity analysis for aerodynamic optimization: A survey of approaches, *Computers & Fluids*, Vol. 39, No. 3, 2010, pp. 373-391.

[3] Choi, K. and Kim, N., Structural Sensitivity Analysis and Optimization, Vol. 1, *Springer Science + Business Media*, 2005.

[4] Etienne, S. and Pelletier, D., A general approach to sensitivity analysis of fluid-structure interactions, *Journal of fluids and structures*, Vol. 21, No. 2, 2005, pp. 169-186.

[5] Liu, S. and Canfield, R. A., Boundary velocity method for continuum shape sensitivity of nonlinear fluidstructure interaction problems, *Journal of Fluids and Structures*, Vol. 40, No. 0, 2013, pp. 284-301.

[6] Hicken, J. E. and Zingg, D. W., Aerodynamic optimization algorithm with integrated geometry parameterization and mesh movement, *AIAA Journal*, Vol. 48, No. 2, 2010, pp. 400-413.

[7] Mittal, R. and Iaccarino, G., Immersed boundary methods, *Annu. Rev. Fluid Mech.*, Vol. 37, 2005, pp. 239-261.

[8] Gobal, K., Grandhi, R. V., and Kolonay, R. M., Continuum Sensitivity Analysis for Structural Shape Design Variables Using Finite-Volume Method, *AIAA Journal*, Vol. 53, No. 2, 2015, pp. 347-355.

[9] Deaton, J. D. and Grandhi, R. V., A survey of structural and multidisciplinary continuum topology optimization: post 2000, *Structural and Multidisciplinary Optimization*, Vol. 49, No. 1, 2014, pp. 1-38.